HAL open science

Generalized Correlation Profiles in Single-File Systems

Alexis Poncet, Aurélien Grabsch, Pierre Illien, Olivier Bénichou

To cite this version:

Alexis Poncet, Aurélien Grabsch, Pierre Illien, Olivier Bénichou. Generalized Correlation Profiles in Single-File Systems. Physical Review Letters, 2021, 127 (22), pp.220601. 10.1103/PhysRevLett.127.220601 . hal-03446060

HAL Id: hal-03446060

https://hal.science/hal-03446060v1

Submitted on 24 Nov 2021

HAL is a multi-disciplinary open access archive for the deposit and dissemination of scientific research documents, whether they are published or not. The documents may come from teaching and research institutions in France or abroad, or from public or private research centers.

L'archive ouverte pluridisciplinaire **HAL**, est destinée au dépôt et à la diffusion de documents scientifiques de niveau recherche, publiés ou non, émanant des établissements d'enseignement et de recherche français ou étrangers, des laboratoires publics ou privés.

arXiv:2103.13083v2 [cond-mat.stat-mech] 11 Aug 2021

Generalised density profiles in single-file systems

Alexis Poncet,[1] Aurélien Grabsch,[1] Pierre Illien,[2] and Olivier Bénichou[1]

[1] *Sorbonne Université, CNRS, Laboratoire de Physique Théorique de la Matière Condensée (LPTMC), 4 Place Jussieu, 75005 Paris, France*

[2] *Sorbonne Université, CNRS, Laboratoire de Physico-Chimie des Électrolytes et Nanosystèmes Interfaciaux (PHENIX), 4 Place Jussieu, 75005 Paris, France*

(Dated: August 12, 2021)

Single-file diffusion refers to the motion in narrow channels of particles which cannot bypass each other, and leads to tracer subdiffusion. Most approaches to this celebrated many-body problem were restricted to the description of the tracer only. Here, we go beyond this standard description by introducing and providing analytical results for generalised density profiles (GDPs) in the frame of the tracer. In addition to controlling the statistical properties of the tracer, these quantities fully characterise the correlations between the tracer position and the bath particles density. Considering the hydrodynamic limit of the problem, we determine the scaling form of the GDPs with space and time, and unveil a non-monotonic dependence with the distance to the tracer despite the absence of any asymmetry. Our analytical approach provides several exact results for the GDPs for paradigmatic models of single-file diffusion, such as Brownian particles with hardcore repulsion, the Symmetric Exclusion Process and the Random Average Process. The range of applicability of our approach is further illustrated by considering (i) extensions to general interactions between particles, (ii) the out-of-equilibrium situation of an initial step of density and (iii) beyond the hydrodynamic limit, the GDPs at arbitrary time in the dense limit.

The key feature of single-file diffusion [1–3], which refers to the motion of particles which cannot bypass each other, is that a typical displacement of a tracer particle scales as $t^{1/4}$ instead of $t^{1/2}$ as in regular diffusion [4–11]. This subdiffusive scaling has been demonstrated in a growing number of experimental realizations, in contexts as varied as transport in porous media [12, 13], zeolites [14] or confined colloidal suspensions [15, 16]. Theoretically, it has lead to a huge number of works in the physical and mathematical literature. Recent advances include the determination of the large deviation functions of the position of a tracer in a system of Brownian particles with hardcore repulsion [17–19] and in the Symmetric Exclusion Process [20, 21] (see below for definitions), which are two paradigmatic models of single-file diffusion with hard-core interactions.

Theoretical interest in single-file diffusion originates from the challenging many-body nature of the problem: any large displacement of the tracer particle in one direction requires large displacements of more and more bath particles in the same direction. However, the quantification of the coupling between the tracer position and the bath particles density remains a broadly open question. Here, we develop a theoretical framework with which to determine these correlations for single-file systems.

We introduce our formalism by considering first the Symmetric Exclusion Process (SEP). Particles, present at a density ρ, perform symmetric continuous-time random walks on a one-dimensional lattice with unit jump rate, and hard-core exclusion is enforced by allowing at most one particle per site (Fig. 1(a)). The tracer, of position X_t at time t, is initially at the origin. The bath particles are described by the set of occupation numbers $\eta_r(t)$ of each site $r \in \mathbb{Z}$ of the line at time t, with $\eta_r(t) = 1$ if the site is occupied and $\eta_r(t) = 0$ otherwise.

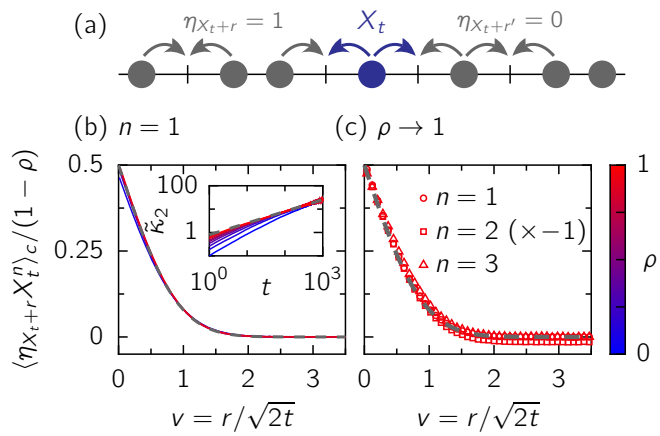

FIG. 1. SEP. (a) The Symmetric Exclusion Process (SEP). The position of the tracer is called X_t and the occupation numbers of the sites with respect to the tracer are denoted η_{X_t+r}. (b) Profiles of order 1 at densities $0.1, 0.25, 0.5, 0.75, 0.9$ at time $t = 3000$ (blue to red). Dashed gray line: prediction from Eq. (9). Inset: rescaled variance $\tilde{\kappa}_2 = \kappa_2\rho/(1-\rho)$ compared to known expression (gray) [7] and retrieved by our approach. (c) Profiles of order 1, 2 and 3 at high density ($\rho = 0.95, t = 1000$). Dashed gray line: prediction from Eq. (10).

To quantify the coupling between the position of the tracer and the density of bath particles, we study the joint process (X_t, η_{X_t+r}), which is entirely characterized by its joint cumulant generating function $\ln\langle e^{\lambda X_t + \chi \eta_{X_t+r}}\rangle$. Since η_{X_t+r} only takes values 0 and 1, this function takes the form

$$\ln\langle e^{\lambda X_t + \chi \eta_{X_t+r}}\rangle = \psi(\lambda, t) + \ln(1 + (e^{\chi} - 1) w_r(\lambda, t)), \quad (1)$$

where $\psi(\lambda,t)$ is the usual cumulant-generating function, whose expansion defines the cumulants κ_n of the position:

$$\psi(\lambda,t) \equiv \ln\left\langle e^{\lambda X_t}\right\rangle \equiv \sum_{n=1}^{\infty}\frac{\lambda^n}{n!}\kappa_n(t). \tag{2}$$

In turn, $w_r(\lambda,t)$ is the GDP-generating function [22] [23].

$$w_r(\lambda,t) = \langle \eta_{X_t+r} e^{\lambda X_t}\rangle / \langle e^{\lambda X_t}\rangle, \tag{3}$$

whose expansion gives the joint cumulants $\langle \eta_{X_t+r} X_t^n\rangle_c$ of the tracer position X_t and the occupation number η_{X_t+r} measured in its frame of reference. For instance, the first cumulant $\langle \eta_{X_t+r} X_t\rangle_c = \mathrm{Cov}(\eta_{X_t+r}, X_t)$ provides a measure of the correlations between the displacement of the tracer and the occupation of the site at a distance r of the tracer, while the second one $\langle \eta_{X_t+r} X_t^2\rangle_c = \mathrm{Cov}(\eta_{X_t+r}, X_t^2)$ (since $\langle X_t\rangle$=0) gives a measure of the correlation between the amplitude of the fluctuations of X_t and the occupation at a distance r of X_t. Finally, the joint cumulant generating function $\ln\langle e^{\lambda X_t + \chi \eta_{X_t+r}}\rangle$ is given by the knowledge of ψ and w_r, which are thus key quantities, whose joint determination is the object of this Letter.

While it is known that the cumulant-generating function ψ scales as $\sqrt{t}$ at large time for single-file systems, we put forward that, more generally, at large scale (large time, large distances), the GDP-generating function admits the scaling form:

$$w_r(\lambda,t) - \rho \underset{t\to\infty}{\sim} \Phi\left(\lambda, v = \frac{r}{\sqrt{2t}}\right) \equiv \sum_{n=1}^{\infty}\frac{\lambda^n}{n!}\Phi_n(v). \tag{4}$$

We note that the symmetry of the system imposes $\Phi(\lambda,v) = \Phi(-\lambda,-v)$: in the following the results will be stated only for $v>0$. When the tracer moves, it perturbs the bath particles and gives birth to density profiles which, as displayed by this scaling form, are not stationary but involve typical length scales growing as $\sqrt{t}$. In turn, the way the bath particles readjust at the front and behind the tracer (encoded in $w_{\pm 1}$) controls its displacement, leading to (see Supplementary Material, SM [24])

$$\frac{\mathrm{d}\psi}{\mathrm{d}t} = \frac{1}{2}\left[(e^{\lambda}-1)(1-w_1) + (e^{-\lambda}-1)(1-w_{-1})\right]. \tag{5}$$

Finally, besides fully quantifying the correlations between the tracer position and the density of bath particles, the GDPs control the time evolution of the cumulant-generating function. In particular, the scaling $\psi(\lambda,t) \underset{t\to\infty}{\sim} \sqrt{t}$ of the cumulants [20, 21] actually originates from the scaling form (4) of the GDP generating-function. Relying on a mixed Eulerian (for the bath particles) and Lagrangian (for the tracer) master equation and on the scaling of Φ (Eq. (4)), we show in SM that this key observable satisfies the hydrodynamic equation

$$\Phi''(v) + 2(v+b_\mu)\Phi'(v) + C(v) = 0 \tag{6}$$

completed by the boundary conditions

$$\Phi'(0^{\pm}) + 2b_{\pm}[\rho + \Phi(0^{\pm})] = 0 \tag{7}$$

$$1-\rho-\Phi(0^-) = e^{\lambda}(1-\rho-\Phi(0^+)) \tag{8}$$

in front and past the tracer, with μ the sign of v, $b_\mu(\lambda) \equiv \lim_{t\to\infty}\psi(\lambda,t)/[\sqrt{2t}(e^{\mu\lambda}-1)]$ and the dependence on λ omitted for simplicity. Equation (8) comes from the cancellation of $\frac{\mathrm{d}\psi}{\mathrm{d}t}$ at large times (see Eq. (5)). The function $C(v)$ involves higher order correlations, and is *a priori* unknown. However, as we report below (see SM for details), explicit exact expressions of the GDPs can be obtained in several important situations.

First, we show that the function $C(v)$ is strictly equal to zero at first order in λ, making the equation (6) closed at this order, and leading to

$$\Phi_1(v>0) = \frac{1-\rho}{2}\,\mathrm{erfc}(v). \tag{9}$$

This expression provides the exact large-time behavior of the correlation function $\langle \eta_{X_t+r} X_t\rangle_c = \mathrm{Cov}(\eta_{X_t+r}, X_t)$ of the SEP at any density. The fact that it is positive for $v>0$ indicates that, if $X_t>0$, the sites to the right of the tracer have higher occupation numbers, which shows that there is an accumulation of particles in front of the tracer. Note that it decays monotonically to zero with the distance to the tracer (Fig. 1(b)). We finally stress that (9) together with (8) allows one to recover in a straightforward way the well known expression of the second cumulant $\kappa_2(t) = (1-\rho)/\rho\sqrt{2t/\pi}$ [4].

Second, in the dense limit $\rho\to 1$, it is shown that the function $C(v)$, which involves a product of occupation numbers of bath particles, vanishes, which leads to the full GDP-generating function

$$\lim_{\rho\to 1}\frac{\Phi(\lambda, v>0)}{1-\rho} = \frac{1-e^{-\lambda}}{2}\,\mathrm{erfc}(v), \tag{10}$$

where the dependencies on λ and v factorise. This expression gives the GDPs of arbitrary order, which, up to a sign, assume all the same value, and again decay monotonically to zero (Fig. 1(c)).

Third we investigate the dilute limit $\rho\to 0$ of the SEP. We stress that the results in this case cannot be deduced from the dense limit discussed above, since the particle-hole symmetry of the SEP is explicitly broken by choosing to follow the motion of one particle. Actually, this limits exhibits a richer phenomenology. In fact, it corresponds to the model of interacting point-like particles on a line [17–19], and needs to be taken at constant $x=\rho r$ and $\tau = \rho^2 t$. The density field $\eta_{X_t+r}(t) \mapsto \eta(x,\tau)$ becomes continuous in space and the diffusive scaling for the GDPs reads $v = r/\sqrt{2t} = x/\sqrt{2\tau}$, leading to the definition $\hat{\Phi}(\hat{\lambda},v) = \lim_{\rho\to 0}[\Phi(\lambda=\rho\hat{\lambda},v)/\rho]$. In this case, the function $C(v)$ is not negligible, but we put forward self-consistently, in order to retrieve the known

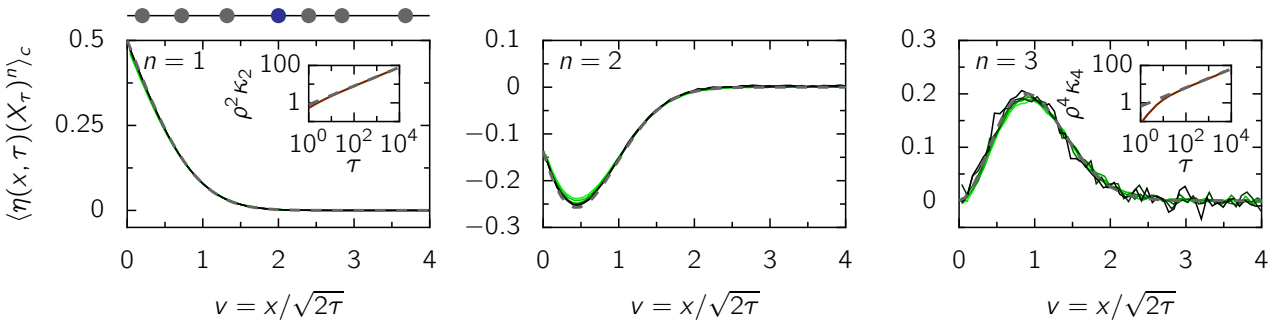

FIG. 2. Pointlike interacting particles. Rescaled orders 1, 2 and 3 (left to right) of the GDPs at times $\tau = 100, 200, 500, 1000, 2000, 5000$ (green to black). The dashed gray lines are the predictions from Eqs. (9), (15), (16). The insets show the second and fourth cumulants with the solid lines corresponding to the simulations and the dashed gray line to the solution from Eq. (14).

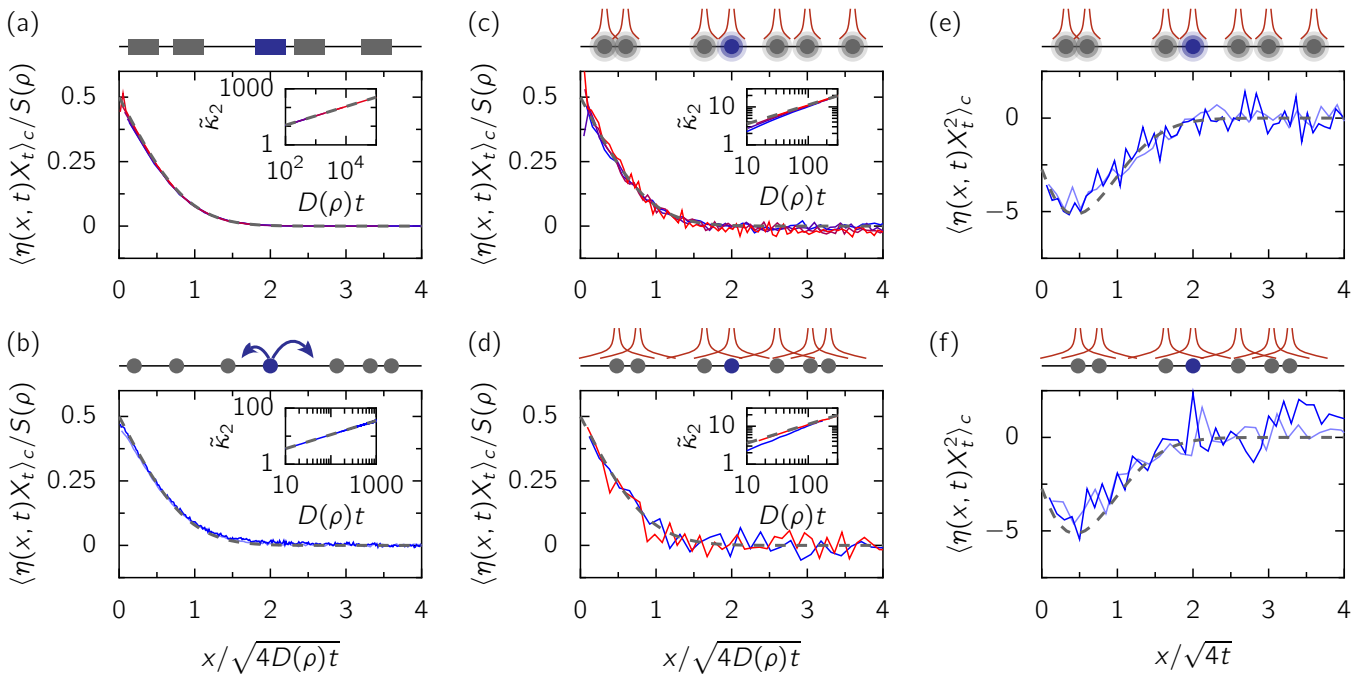

FIG. 3. GDPs of single-file systems. (a-d) Profiles at order 1 for various models. The dashed gray lines correspond to the prediction of Eq. (17). The insets show the rescaled variance $\tilde\kappa_2 = \kappa_2\rho/S(\rho)$ with the prediction in gray. (a) Hard-rod gas at density $\rho = 1$ and time $t = 1000$. The length of a rod is $a = 0.1, 0.25, 0.5, 0.75, 0.9$ (blue to red). The parameters are $S(\rho) = (1-a\rho)^2$, $D(\rho) = (1-a\rho)^{-2}$ [16]. (b) Random-average process [25, 26] at density $\rho = 1$ at times $t = 1000$ and 5000 (light blue and blue): at exponential times, each particle performs a symmetric jump whose length is a random fraction of the distance to the nearest particle. $S(\rho)$ and $D(\rho)$ are given in Ref. [26]. (c) Point-like Brownian particles interacting by a Weeks-Chandler-Andersen potential ($V(r) \propto (\frac{1}{r^{12}} - \frac{1}{r^6})$ for $r < 2^{1/6}$ and 0 otherwise). Density $\rho = 0.2, 0.3, 0.4, 0.5$ (blue to red) at time $t = 100$. $S(\rho)$ is the structure factor at vanishing wave-number, and $D(\rho) = D_0/S(\rho)$ [16, 27]. (d) Point-like Brownian particles interacting with long-range dipole-dipole interactions $V(r) \propto \frac{1}{r^3}$ at density $\rho = 0.2$ and 0.4 (blue and red) at time $t = 100$. (e-f) Profiles of order 2 for the same models as (c-d) at density $\rho = 0.05$ and times $5\cdot 10^3$ and $1\cdot 10^4$ (light blue and blue). The dashed gray line is the low-density prediction from Eq. (15).

cumulants κ_n (see point (i) below), the closure relation

$$\lim_{\rho\to 0}[C(\lambda = \rho\hat\lambda, v)/\rho] = 2\hat\lambda\frac{d\beta}{d\hat\lambda}\hat\Phi'(v), \tag{11}$$

where we defined $\beta = \lim_{t\to\infty}\frac{1}{\sqrt{2t}}\frac{\hat\psi}{\hat\lambda}$, with $\hat\psi(\hat\lambda) = \lim_{\rho\to 0}[\psi(\lambda = \rho\hat\lambda)/\rho]$. This leads to the key and strikingly simple closed equation for the full GDP-generating function

$$\hat\Phi''(v) + 2(v+\xi)\hat\Phi'(v) = 0, \tag{12}$$

which is the main result of this Letter. It yields

$$\hat{\Phi}(\hat{\lambda}, v>0) = \frac{\beta \operatorname{erfc}(v+\xi)}{\pi^{-1/2}e^{-\xi^2} - \beta \operatorname{erfc}(\xi)}. \tag{13}$$

where $\xi = \lim_{t\to\infty} \frac{1}{\sqrt{2t}} \frac{d\hat{\psi}}{d\hat{\lambda}}$. The quantities β and $\xi = \frac{d}{d\hat{\lambda}}(\hat{\lambda}\beta)$ are then determined from Eq. (8), which becomes

$$\beta \sum_{\mu=\pm 1} \frac{\operatorname{erfc}(\mu\xi)}{\pi^{-1/2}e^{-\xi^2} - \mu\beta \operatorname{erfc}(\mu\xi)} = \hat{\lambda}. \tag{14}$$

Several comments are in order. (i) Eq. (14) is an implicit equation that allows one to retrieve the exact cumulants κ_n obtained in previous studies [17–19] (see SM [24] for detailed correspondence). This validates self-consistently the closure relation (11). (ii) Then, Eq. (13) provides the GDPs of interacting point-like particles at arbitrary order; for instance (Fig. 2),

$$\Phi_2(v) = \frac{1}{\rho}\left[\frac{1}{2}\operatorname{erfc} v - 2\frac{e^{-v^2}}{\pi}\right], \tag{15}$$

$$\Phi_3(v) = \frac{3}{\pi^{3/2}\rho^2}\left[(2v-\sqrt{\pi})e^{-v^2} + \sqrt{\pi}\operatorname{erfc} v\right]. \tag{16}$$

(iii) The sign of these GDPs is non trivial. For instance, $\Phi_2(v) = \mathrm{Cov}(\eta_{X_t+r}, X_t^2)$ is negative (see Fig. 2 for $n=2$), which implies that X_t^2 and η_{X_t+r} fluctuate in opposite directions: a larger fluctuation of X_t^2 is associated with a smaller value of the occupation. Furthermore, even if there is no asymmetry in the dynamics, these GDPs display a surprising non-monotonic behavior with the distance to the tracer (see Fig. 2 for $n \geq 2$), which indicates that this effect is more pronounced at a certain distance of the tracer (which is non stationary, and grows as $\sqrt{t}$). (iv) It is demonstrated in SM [24] that the GDPs actually coincide with the saddle-point solution in the formalism of Macroscopic Fluctuation Theory [28], evaluated at a specific point. In turn, it sheds new light on this saddle-point solution. This, after (i), is a further validation of the exactness of the closure relation (11). A key result of our approach is that the GDPs satisfy the very simple closed equation (12). (v) We stress that our approach can be generalized to the important out-of-equilibrium situation of an initial step of density [21, 29]. The main equation (12) remains valid in this case, and only the boundary conditions (7,8) must be straightforwardly adapted. The modified equations, and explicit expressions of the cumulants and the GDPs are given in SM [24] (Eqs. (S55-S62)).

These analytical results can also be extended to a general single-file system of interacting particles with average density ρ. Such a system can be described at large scale by two quantities: the collective diffusion coefficient $D(\rho)$ and the static structure factor at vanishing wavenumber $S(\rho)$ [16, 27, 30]. The case of the SEP considered above corresponds to $D(\rho) = 1/2$ and $S(\rho) = 1-\rho$. We conjecture that the first-order GDP of a general single-file system can be obtained by adapting the main equation (12) into $D(\rho)\Phi_1''(v) + v\Phi_1'(v) = 0$, with the boundary conditions $2D(\rho)\Phi_1'(0^\pm) + \rho\tilde{\kappa}_2 = 0$ and $\Phi_1(0^+) - \Phi_1(0^-) = S(\rho)$. This leads to the general expression

$$\Phi_1(v \geq 0) = \frac{S(\rho)}{2}\operatorname{erfc}\left(\frac{v}{\sqrt{2D(\rho)}}\right). \tag{17}$$

Note that the known expression of the variance of the tracer $\kappa_2(t) = (S(\rho)/\rho)\sqrt{4D(\rho)t/\pi}$ [27, 30] is recovered from the particular value $\Phi_1(0)$. The analytical result (17) can be retrieved by a MFT computation provided in SM [24]. Furthermore, it is supported by numerical simulations (Fig. 3) of several paradigmatic examples of single-file systems (see SM [24] for definitions) with hard-core interactions (the Brownian hard-rods model, Fig. 3(a), as involved in the experimental realisation of the quasi-1D colloidal suspension from [16], and the random average process, Fig. 3(b) [25, 26, 31, 32]) and more general pairwise interactions (Brownian point-like particles with Weeks-Chandler-Anderson (WCA) potential Fig. 3(c), and dipole-dipole interactions, Fig. 3(d), as involved in the experimental realisation of paramagnetic colloids confined in a 1D channel from [15]).

Higher order GDPs can also be obtained in the dilute limit. Indeed, in the limit $\rho \to 0$ of a generic single-file system, the collective diffusion coefficient and the structure factor should respectively satisfy $D(\rho) \to D_0$ and $S(\rho) \to 1$ where D_0 is the diffusion constant of an individual particle and 1 is the structure factor of the ideal gas. Equations (13)-(16) are therefore valid for such a system at low enough density, as confirmed by numerical simulations (Fig. 3(e)-(f)).

Although we mostly focused on the hydrodynamic limit, we stress that our approach also provides a framework to analyse the GDP-generating function (3) at all times. Starting from the microscopic equation satisfied by w_r (see Eq.(S66)-(S68) in SM), the dense limit of the GDP-generating function $\check{w}_r = \lim_{\rho\to 1}(w_r - \rho)/(1-\rho)$ in the Laplace domain reads

$$\tilde{w}_r(u) = \int_0^\infty e^{-ut}\check{w}_r(t)dt = \frac{1}{u}\frac{1-e^{-\nu\lambda}}{1+\alpha}\alpha^{|r|}, \tag{18}$$

where $\nu = \operatorname{sign} r$ and $\alpha = 1 + u - \sqrt{(1+u)^2 - 1}$, and the dense limit of the cumulant generating function at all times $\check{\psi}(\lambda, t) = \lim_{\rho\to 1}\psi/(1-\rho) = te^{-t}(I_0(t) + I_1(t))[\cosh\lambda - 1]$, where I_n is a modified Bessel function of order n.

All together, the theoretical framework developed in this Letter allows one to quantify the correlations between the tracer and the bath of particles in single-file diffusion with the help of generalized density profiles. We emphasize the main merits of this method. First,

it is based on a master equation, which is a natural tool for physicists. Second, in the limits considered here, it reduces to a simple first order linear differential equation. In views of the complexity of available methods to study tracer diffusion in single-file systems, such as coupled nonlinear partial differential equation for the Macroscopic Fluctuation Theory [17, 28] or integrable probabilities and Bethe ansatz [21], this is an important simplification. Furthermore, we discover a closure relation which allows to break the infinite hierarchy in a many-body model of point-like particles with hardcore repulsion. Beyond these technical aspects, the impact of the present results is further demonstrated by considering extensions to general interactions between particles, the out-of-equilibrium situation of an initial step of density and, beyond the hydrodynamic limit, the GDPs at arbitrary time in the dense limit. Finally, our method opens the way to the resolution at arbitrary density, which is a long-standing and challenging question. As a first step in this direction, we emphasize that the boundary equation (7) remarkably holds at *any* density.

[1] T. Chou, K. Mallick, and R. K. P. Zia, Reports on Progress in Physics **74**, 116601 (2011).

[2] K. Mallick, Physica A: Statistical Mechanics and its Applications **418**, 17 (2015).

[3] P. Krapivski, S. Redner, and E. Ben-Naim, *A Kinetic View of Statistical Physics* (Cambridge University Press, 2009).

[4] T. E. Harris, Journal of Applied Probability **2**, 323 (1965).

[5] D. G. Levitt, Physical Review A **8**, 3050 (1973).

[6] S. Alexander and P. Pincus, Physical Review B **18**, 2011 (1978).

[7] R. Arratia, The Annals of Probability **11**, 362 (1983).

[8] C. Rödenbeck, J. Kärger, and K. Hahn, Physical Review E **57** (1998).

[9] A. Taloni and M. A. Lomholt, Physical Review E **78**, 051116 (2008).

[10] A. Taloni, A. Chechkin, and J. Klafter, Phys. Rev. E **84**, 021101 (2011).

[11] A. Taloni and F. Marchesoni, Biophysical Reviews and Letters **09**, 381 (2014), https://doi.org/10.1142/S1793048014400050.

[12] V. Gupta, S. S. Nivarthi, A. V. McCormick, and H. Ted Davis, Chemical Physics Letters **247**, 596 (1995).

[13] T. Meersmann, J. W. Logan, R. Simonutti, S. Caldarelli, A. Comotti, P. Sozzani, L. G. Kaiser, and A. Pines, The Journal of Physical Chemistry A **104**, 11665 (2000).

[14] K. Hahn, J. Kärger, and V. Kukla, Physical Review Letters **76**, 2762 (1996).

[15] Wei, Bechinger, and Leiderer, Science **287**, 625 (2000).

[16] B. Lin, M. Meron, B. Cui, S. A. Rice, and H. Diamant, Physical Review Letters **94**, 216001 (2005).

[17] P. L. Krapivsky, K. Mallick, and T. Sadhu, Physical Review Letters **113**, 078101 (2014).

[18] C. Hegde, S. Sabhapandit, and A. Dhar, Phys. Rev. Lett. **113**, 120601 (2014).

[19] T. Sadhu and B. Derrida, Journal of Statistical Mechanics: Theory and Experiment **2015**, P09008 (2015).

[20] P. Illien, O. Bénichou, C. Mejía-Monasterio, G. Oshanin, and R. Voituriez, Physical Review Letters **111**, 038102 (2013).

[21] T. Imamura, K. Mallick, and T. Sasamoto, Physical Review Letters **118**, 160601 (2017).

[22] P. Illien, O. Bénichou, G. Oshanin, and R. Voituriez, J. Stat. Mech. , P11016 (2015).

[23] Note that the GDP-generating function (3) can be thought as the average occupation in a biaised ensemble. This type of objects has received a lot of attention over the last years [33–35].

[24] Supplementary Material available at....

[25] R. Rajesh and S. N. Majumdar, Physical Review E **64**, 036103 (2001).

[26] A. Kundu and J. Cividini, EPL (Europhysics Letters) **115**, 54003 (2016).

[27] M. Kollmann, Physical Review Letters **90**, 4 (2003).

[28] P. L. Krapivsky, K. Mallick, and T. Sadhu, Journal of Statistical Physics **160**, 885 (2015).

[29] B. Derrida and A. Gerschenfeld, Journal of Statistical Physics **136**, 1 (2009).

[30] P. L. Krapivsky, K. Mallick, and T. Sadhu, Journal of Statistical Mechanics: Theory and Experiment **2015**, P09007 (2015).

[31] P. Ferrari and L. Fontes, Electronic Journal of Probability **3**, 1 (1998).

[32] G. M. Schütz, Journal of Statistical Physics **99**, 1045 (2000).

[33] H. Touchette, Journal of Statistical Physics **159**, 987 (2015).

[34] R. Chetrite and H. Touchette, Annales Henri Poincaré **16**, 2005 (2015).

[35] B. Derrida and T. Sadhu, Journal of Statistical Physics **176**, 773 (2019).

arXiv:2103.13083v2 [cond-mat.stat-mech] 11 Aug 2021

Generalised density profiles in single-file systems
Supplementary Material

CONTENTS

I. Equations 1
- A. Master equation of the SEP 1
- B. Observables and large-times scalings 2
- C. Equations at arbitrary time 2
- D. Hydrodynamic equations at large time 3

II. Results 3
- A. First order 3
- B. High density 3
- C. Low density 4
- D. Initial step density in the dilute limit 5
- E. Solution at all times in the high density limit 6

III. Generic single-file systems 7
- A. Description of single-file systems in terms of two quantities 7
- B. Extension of our approach 8
- C. MFT 9

IV. Numerical simulations 11
- A. Symmetric exclusion principle 11
- B. Point-like hard-core diffusive particles 11
- C. Hard-rod gas 11
- D. Random-average process 11
- E. Point-like particles interacting by a pairwise potential 12

References 12

I. EQUATIONS

A. Master equation of the SEP

We consider the symmetric exclusion process (SEP) with a tracer. The position of the tracer is denoted X and the configuration of the system is denoted $\underline{\eta} = \{\eta_r\}_{r\in\mathbb{Z}}$ where $\eta_r \in \{0,1\}$ is the occupation of site r (1 if the site is occupied, 0 if it is empty). At time t, the system is characterized by a probability law $P(X,\underline{\eta},t)$.

The initial conditions are given by the equilibrium probability law for the occupations with the tracer at position 0,

$$P(X,\underline{\eta},0) = \delta_{X,0}\delta_{\eta_0,1}\prod_{r\in\mathbb{Z}^*}\delta_{\eta_r,\gamma_r}. \tag{S1}$$

where γ_r are independent Bernouilli variables with parameter ρ (density of the system).

One checks that the time-evolution of the tracer and the bath is given by the following master equation,

$$\begin{aligned}\partial_t P(X,\underline{\eta},t) = &\frac{1}{2}\sum_{r\neq X,X-1}\left[P(X,\underline{\eta}^{r,+},t) - P(X,\underline{\eta},t)\right]\\ &+\frac{1}{2}\sum_{\mu=\pm1}\left\{(1-\eta_X)P(X-\mu,\underline{\eta},t) - (1-\eta_{X+\mu})P(X,\underline{\eta},t)\right\}.\end{aligned} \tag{S2}$$

The first term corresponds to the jumps of the bath particles while the second one takes into account the jumps of the tracer. We call $\underline{\eta}^{r,+}$ the configuration $\underline{\eta}$ in which the occupations of sites r and $r+1$ are exchanged.

If one considers an observable $O(X,\underline{\eta})$, its average at time t is defined as

$$\langle O\rangle(t) \equiv \sum_{X,\underline{\eta}} O(X,\underline{\eta})P(X,\underline{\eta},t). \tag{S3}$$

The time evolution of this average can be computed using the master equation (S2).

B. Observables and large-times scalings

The first observable that we compute is the cumulant-generating function of the displacement of the tracer,

$$\psi(\lambda,t) \equiv \ln\left\langle e^{\lambda X}\right\rangle. \tag{S4}$$

Its expansion in powers of λ generates the cumulants of the tracer. At large time t, it scales as $\sqrt{t}$,

$$\psi(\lambda,t) \underset{t\to\infty}{\sim} A(\lambda)\sqrt{2t}. \tag{S5}$$

The second observable corresponds to the generalized profiles,

$$w_r(\lambda,t) \equiv \frac{\langle \eta_{X+r}e^{\lambda X}\rangle}{\langle e^{\lambda X}\rangle}. \tag{S6}$$

The expansion in powers of λ gives the cross-cumulants between the occupations and the displacement of the tracer. At large time, they satisfy a diffusive scaling $r/\sqrt{t}$,

$$w_r(\lambda,t) - \rho \underset{t\to\infty}{\sim} \Phi\left(v=\frac{r}{\sqrt{2t}},\lambda\right) \tag{S7}$$

Finally, we consider the "modified centered correlations",

$$f_{\mu,r}(\lambda,t) \equiv \frac{\left\langle (1-\eta_{X+\mu})\eta_{X+r}e^{\lambda X}\right\rangle}{\langle e^{\lambda X}\rangle} - \begin{cases}(1-w_\mu)w_{r-\mu} & \text{if } \mu r>0\\ (1-w_\mu)w_r & \text{if } \mu r<0\end{cases}. \tag{S8}$$

At large time, the leading term is in $t^{-1/2}$ and the sub-leading term in t^{-1} with the same diffusive scaling as for the profiles,

$$f_{\mu,r}(\lambda,t) = \frac{1}{\sqrt{2t}}F_\mu\left(v=\frac{r}{\sqrt{2t}},\lambda\right) + \frac{1}{2t}G_\mu\left(v=\frac{r}{\sqrt{2t}},\lambda\right) + \mathcal{O}(t^{-3/2}). \tag{S9}$$

C. Equations at arbitrary time

Using Eqs. (S2) and (S3), one obtains the following equations for the time-evolution of the cumulant-generating function and of the generalized profiles.

$$\partial_t\psi = \frac{1}{2}\left\{(e^{\lambda}-1)(1-w_1)+(e^{-\lambda}-1)(1-w_{-1})\right\}, \tag{S10}$$

$$\partial_t w_r = \frac{1}{2}\Delta w_r - B_\nu\nabla_{-\nu}w_r + \frac{1}{2}\sum_{\mu=\pm1}\left(e^{\mu\lambda}f_{\mu,r+\mu} - f_{\mu,r}\right) \qquad (r\neq\pm1) \tag{S11}$$

$$\partial_t w_{\pm1} = \frac{1}{2}\nabla_\pm w_{\pm1} + B_\pm w_{\pm1} + \frac{1}{2}\left(e^{\pm\lambda}f_{\pm1,\pm2} - f_{\mp1,\pm1}\right) \tag{S12}$$

ν is the sign of r, the gradients are $\nabla_\mu u_r = u_{r+\mu} - u_r$, and

$$B_\pm = \frac{\partial_t\psi}{e^{\pm\lambda}-1}. \tag{S13}$$

In addition to that, the generalized profiles at large distance are equal to the density $\lim_{r\to\pm\infty} w_r = \rho$.

D. Hydrodynamic equations at large time

Using the time scalings of subsection I B into the equations of subsection I C, we first obtain two "symmetry" relations

$$1-\rho-\Phi(0^-)=e^{\lambda}(1-\rho-\Phi(0^+)), \tag{S14}$$

$$F_{-1}(v)=e^{\lambda}F_1(v). \tag{S15}$$

Then, we obtain the following hydrodynamic equations for the generalized profiles,

$$\Phi''(v)+2(v+b_\nu)\Phi'(v)+C(v)=0, \tag{S16}$$

$$C(v)=(e^{\lambda}-1)F_1'(v)+\sum_{\mu=\pm1}(e^{\mu\lambda}-1)G_\mu(v) \tag{S17}$$

$$\Phi'(0^\pm)+2b_\pm[\rho+\Phi(0^\pm)]=0, \tag{S18}$$

$$\Phi(v)\xrightarrow[v\to\pm\infty]{}0, \tag{S19}$$

with ν the sign of v and $b_\pm(\lambda)=\sqrt{2t}B_\pm(\lambda)=\pm A(\lambda)/(e^{\pm\lambda}-1)$.

II. RESULTS

A. First order

At order 1 in λ, $\Phi(\lambda,v)=\lambda\Phi_1(v)+\mathcal{O}(\lambda^2)$ and $b_\pm=\lambda\tilde{\kappa}_2/2+\mathcal{O}(\lambda^2)$ with $\hat{\kappa}_2=[\langle X^2(t)\rangle-\langle X(t)\rangle^2]/\sqrt{2t}$. Equations (S14), (S16), (S18) and (S19) lead to

$$\Phi_1''(v)+2v\Phi_1'(v)=0, \tag{S20}$$

$$\Phi_1'(0^\pm)+\rho\tilde{\kappa}_2=0, \tag{S21}$$

$$\Phi_1(0^+)-\Phi_1(0^-)=1-\rho, \tag{S22}$$

$$\Phi_1(v)\xrightarrow[v\pm\infty]{}0. \tag{S23}$$

This set of equations is closed. Its resolution gives the generalized profiles at order 1 and the rescaled variance of the tracer,

$$\Phi_1(v\gtrless0)=\pm\frac{1-\rho}{2}\operatorname{erfc}|v|, \tag{S24}$$

$$\tilde{\kappa}_2=\frac{1-\rho}{\rho}\frac{1}{\sqrt{\pi}}. \tag{S25}$$

The result for the variance is the well-known one [1].

B. High density

We now turn to the high density limit $\rho\to1$. We define the following quantities (that no longer depend on the density),

$$\check{\Phi}(v)=\lim_{\rho\to1}\frac{\Phi(v)}{1-\rho},\qquad \check{b}_\pm=\lim_{\rho\to1}\frac{b_\pm}{1-\rho}. \tag{S26}$$

Equations (S14), (S16), (S18) and (S19) simplify into

$$\check{\Phi}''(v)+2v\check{\Phi}'(v)=0, \tag{S27}$$

$$\check{\Phi}_1'(0^\pm)+2\check{b}_\pm=0, \tag{S28}$$

$$e^{\lambda}[1-\check{\Phi}(0^+)]=1-\check{\Phi}(0^-), \tag{S29}$$

$$\check{\Phi}(v)\xrightarrow[v\pm\infty]{}0. \tag{S30}$$

The set of equations is closed and leads to

$$\check{\Phi}(v \gtrless 0) = \frac{1}{2}(1 - e^{\mp\lambda}) \operatorname{erfc}|v|, \tag{S31}$$

$$\check{\psi}(\lambda) \underset{t\to\infty}{\sim} \sqrt{\frac{2t}{\pi}} \left[\cosh\lambda - 1\right]. \tag{S32}$$

We recover the cumulant-generating function of Ref. [6].

C. Low density

The opposite limit of low density, $\rho \to 0$, is trickier to define. One should consider it keeping $z = \rho r$ and $\tau = \rho^2 t$ constant. With these scalings, one realizes that the correct limits are

$$\hat{\Phi}(v, \hat{\lambda}) = \lim_{\rho\to 0} \frac{\Phi(v, \lambda = \rho\hat{\lambda})}{\rho}, \qquad \beta(\hat{\lambda}) = \lim_{\rho\to 0} \frac{\pm b_\pm(\lambda = \rho\hat{\lambda})}{\rho} = \lim_{\rho\to 0} \frac{A(\lambda = \rho\hat{\lambda})}{\rho\hat{\lambda}}, \tag{S33}$$

$$\hat{F}_\mu(v, \hat{\lambda}) = \lim_{\rho\to 0} \frac{F_\mu(v, \lambda = \rho\hat{\lambda})}{\rho}, \qquad \hat{G}_\mu(v, \hat{\lambda}) = \lim_{\rho\to 0} G_\mu(v, \lambda = \rho\hat{\lambda}). \tag{S34}$$

$$\tag{S35}$$

The bulk equation (S16) gives

$$\hat{\Phi}''(v) + 2(v + \beta)\hat{\Phi}'(v) + \hat{\lambda}\left[\hat{G}_1(v) - \hat{G}_{-1}(v)\right] = 0. \tag{S36}$$

This time the equation is not closed. We put forward the following closure relation,

$$\hat{G}_1(\hat{\lambda}, v) - \hat{G}_{-1}(\hat{\lambda}, v) = 2\frac{d\beta}{d\hat{\lambda}}\hat{\Phi}'(v), \tag{S37}$$

which leads us to

$$\hat{\Phi}''(v) + 2(v + \xi)\hat{\Phi}'(v) = 0, \tag{S38}$$

with ξ the (rescaled) derivative of the cumulant-generating function with respect to its parameter,

$$\xi \equiv \beta + \hat{\lambda}\frac{d\beta}{d\hat{\lambda}} = \frac{d}{d\hat{\lambda}}(\hat{\lambda}\beta) = \frac{d\hat{A}(\hat{\lambda}, \tau)}{d\hat{\lambda}}. \tag{S39}$$

The low density limit of Equations (S14), (S18) and (S19) is readily taken and the set of equations we need to solve is

$$\hat{\Phi}''(v) + 2(v + \xi)\hat{\Phi}'(v) = 0, \tag{S40}$$

$$\hat{\Phi}'(0^\nu) + 2\beta\left[1 + \hat{\Phi}(0^\nu)\right] = 0, \tag{S41}$$

$$\hat{\Phi}(0^+) - \hat{\Phi}(0^-) = \hat{\lambda}, \tag{S42}$$

$$\hat{\Phi}(\pm\infty) = 0. \tag{S43}$$

The computation leads to

$$\hat{\Phi}(v \gtrless 0) = \frac{\pm\beta}{\pi^{-1/2}e^{-\xi^2} \mp \beta \operatorname{erfc}(\pm\xi)} \operatorname{erfc}(\pm(v + \xi)) \tag{S44}$$

Therefore Eq. (S42) yields an implicit equation for β and ξ,

$$\beta\left(\frac{\operatorname{erfc}(\xi)}{\pi^{-1/2}e^{-\xi^2} - \beta\operatorname{erfc}(\xi)} + \frac{\operatorname{erfc}(-\xi)}{\pi^{-1/2}e^{-\xi^2} + \beta\operatorname{erfc}(-\xi)}\right) = \hat{\lambda}. \tag{S45}$$

The coefficients $\hat{\kappa}_1$, $\hat{\kappa}_2$, ... involved in the cumulants are defined by

$$\hat{\Psi}(\hat{\lambda},t) \equiv \sum_{n=1}^{\infty} \frac{\hat{\lambda}^n}{n!}\hat{\kappa}_n\sqrt{2t}, \qquad \beta = \sum_{n=0}^{\infty} \frac{\hat{\lambda}^n}{(n+1)!}\hat{\kappa}_{n+1}, \qquad \xi = \sum_{n=0}^{\infty} \frac{\hat{\lambda}^n}{n!}\hat{\kappa}_{n+1}. \tag{S46}$$

These expressions can be injected into Eq (S45) to obtain the cumulants order by order,

$$\hat{\kappa}_2 = \frac{1}{\sqrt{\pi}}, \qquad \hat{\kappa}_4 = \frac{3(4-\pi)}{\pi^{3/2}}, \tag{S47}$$

$$\hat{\kappa}_6 = \frac{15(68-30\pi+3\pi^2)}{\pi^{5/2}}, \qquad \hat{\kappa}_8 = \frac{21(10912-6840\pi+1320\pi^2-75\pi^3)}{\pi^{7/2}}. \tag{S48}$$

The cumulants are $\kappa_n(t) = \rho^{1-n}\hat{\kappa}_n\sqrt{2t}$. These are exactly the coefficients known in the literature for interacting point-like particles on a line [5, 9, 15], a model which is equivalent to the low density SEP. Furthermore, we are able to give the generalized profiles at all orders in λ,

$$\hat{\Phi}^{(1)}(v) = \frac{1}{2}\operatorname{erfc} v, \tag{S49}$$

$$\hat{\Phi}^{(2)}(v) = \frac{1}{2}\operatorname{erfc} v - 2\frac{e^{-v^2}}{\pi}, \tag{S50}$$

$$\hat{\Phi}^{(3)}(v) = \frac{3}{\pi^{3/2}}\left[(2v-\sqrt{\pi})e^{-v^2} + \sqrt{\pi}\operatorname{erfc} v\right], \tag{S51}$$

$$\hat{\Phi}^{(4)}(v) = -\frac{1}{2\pi^2}\left[(128-24\pi+24\sqrt{\pi}v+32v^2)e^{-v^2} + 3\pi(\pi-8)\operatorname{erfc} v\right]. \tag{S52}$$

D. Initial step density in the dilute limit

Our formalism can be applied to the case of an initial step density with ρ_- for $r<0$ and ρ_+ for $r>0$. At large times, the GDPs take the form

$$w_r(\lambda,t) - \rho_\nu \underset{t\to\infty}{\sim} \Phi\left(v = \frac{r}{\sqrt{2t}}, \lambda\right), \tag{S53}$$

with $\nu = \operatorname{sign}(r)$. We denote $\rho = (\rho_+ + \rho_-)/2$ the mean density and $\hat{\rho}_\pm = \rho_\pm/\rho$. In the dilute limit $\rho \to 0$, we obtain the following set of equations

$$\hat{\Phi}''(v) + 2(v+\xi)\hat{\Phi}'(v) = 0, \tag{S54}$$

$$\hat{\Phi}'(0^\nu) + 2\beta\left[\hat{\rho}_\nu + \hat{\Phi}(0^\nu)\right] = 0, \tag{S55}$$

$$\hat{\Phi}(0^+) - \hat{\Phi}(0^-) + \hat{\rho}_+ - \hat{\rho}_- = \hat{\lambda}, \tag{S56}$$

$$\hat{\Phi}(\pm\infty) = 0. \tag{S57}$$

where $\hat{\Phi}$, β and ξ are defined by Equations (S33) and (S39). This leads to

$$\hat{\Phi}(v \gtrless 0) = \hat{\rho}_\pm \frac{\pm\beta}{\pi^{-1/2}e^{-\xi^2} \mp \beta\operatorname{erfc}(\pm\xi)}\operatorname{erfc}(\pm(v+\xi)). \tag{S58}$$

Therefore Eq. (S56) yields the following implicit equation for β and ξ,

$$\beta\left(\hat{\rho}_+\frac{\operatorname{erfc}(\xi)}{\pi^{-1/2}e^{-\xi^2} - \beta\operatorname{erfc}(\xi)} + \hat{\rho}_-\frac{\operatorname{erfc}(-\xi)}{\pi^{-1/2}e^{-\xi^2} + \beta\operatorname{erfc}(-\xi)}\right) + \hat{\rho}_+ - \hat{\rho}_- = \hat{\lambda}. \tag{S59}$$

We can deduce the coefficients $\hat{\kappa}_1$, $\hat{\kappa}_2$, ... involved in the cumulants by using the expansions of ξ and β (S46). We obtain that $\hat{\kappa}_1$ is solution of

$$\frac{\hat{\rho}_+}{1-\sqrt{\pi}e^{\hat{\kappa}_1^2}\operatorname{erfc}(\hat{\kappa}_1)} = \frac{\hat{\rho}_-}{1+\sqrt{\pi}e^{\hat{\kappa}_1^2}\operatorname{erfc}(-\hat{\kappa}_1)}. \tag{S60}$$

The higher cumulants can be expressed in terms of $\hat{\kappa}_1$. For instance,

$$\hat{\kappa}_2 = \frac{2(1-\sqrt{\pi}\mathrm{e}^{\hat{\kappa}_1^2}\operatorname{erfc}(\hat{\kappa}_1))(1+\sqrt{\pi}\mathrm{e}^{\hat{\kappa}_1^2}\operatorname{erfc}(-\hat{\kappa}_1))}{\hat{\rho}_+(4\hat{\kappa}_1+\sqrt{\pi}(1+4\hat{\kappa}_1^2)\mathrm{e}^{\hat{\kappa}_1^2}\operatorname{erfc}(-\hat{\kappa}_1)) - \hat{\rho}_-(4\hat{\kappa}_1-\sqrt{\pi}(1+4\hat{\kappa}_1^2)\mathrm{e}^{\hat{\kappa}_1^2}\operatorname{erfc}(\hat{\kappa}_1))} \,. \tag{S61}$$

The expressions of $\hat{\kappa}_1$ and $\hat{\kappa}_2$ are identical to the exact ones obtained previously [7, 13] in the dilute limit. In addition to the cumulants, we obtain the expressions of the density profiles at any order, by expanding (S58) in powers of $\hat{\lambda}$. For instance, for $v > 0$,

$$\hat{\Phi}^{(1)}(v) = \frac{\hat{\kappa}_2\hat{\rho}_+\sqrt{\pi}\mathrm{e}^{\hat{\kappa}_1^2}}{2(1-\sqrt{\pi}\mathrm{e}^{\hat{\kappa}_1^2}\hat{\kappa}_1\operatorname{erfc}(\hat{\kappa}_1))^2}\operatorname{erfc}(v+\hat{\kappa}_1) - \frac{2\hat{\kappa}_1\hat{\kappa}_2\hat{\rho}_+}{1-\sqrt{\pi}\mathrm{e}^{\hat{\kappa}_1^2}\hat{\kappa}_1\operatorname{erfc}(\hat{\kappa}_1)}\mathrm{e}^{-v(v+\hat{\kappa}_1)} \,. \tag{S62}$$

E. Solution at all times in the high density limit

In the high density limit $\rho \to 1$, the cumulant-generating function is expected to scale as $(1-\rho)$. We write

$$\psi(\lambda,t) \underset{\rho\to 1}{\sim} (1-\rho)\check{\psi}(\lambda,t), \qquad B_\mu(\lambda,t) \underset{\rho\to 1}{\sim} (1-\rho)\check{B}_\mu(\lambda,t) = (1-\rho)\frac{\partial_t\check{\psi}(\lambda,t)}{e^{\mu\lambda}-1}, \tag{S63}$$

with $\check{\psi}$ and $\check{B}_\mu$ independent of the density ρ.

The fluctuations of occupation $\delta\eta_r = \eta_r - \langle\eta_r\rangle$ also scale as $(1-\rho)$. Thus, the generalized profiles w_r scale as $(1-\rho)$ while the correlations $f_{\mu,r}$ (between $\eta_{X+\mu}$ and η_{X+r}) scale as $(1-\rho)^2$.

$$w_r \underset{\rho\to 1}{\sim} \rho + (1-\rho)\check{w}_r = 1 + (1-\rho)(\check{w}_r - 1), \tag{S64}$$

$$f_{\mu,r} = \mathcal{O}[(1-\rho)^2]. \tag{S65}$$

When all the scalings are written, the microscopic equations (S10)-(S12) become a closed system independent of ρ,

$$\partial_t\check{w}_r = \frac{1}{2}\Delta\check{w}_r \tag{S66}$$

$$\partial_t\check{w}_\mu = \frac{1}{2}\nabla_\mu\check{w}_\mu + \check{B}_\nu(t) \tag{S67}$$

$$\lim_{r\to\pm\infty}\check{w}_r = 0 \tag{S68}$$

$$\partial_t\check{\psi} = \frac{1}{2}\left[(e^\lambda-1)(1-\check{w}_1) + (e^{-\lambda}-1)(1-\check{w}_{-1})\right] \tag{S69}$$

We define the Laplace transform

$$\tilde{w}_r(u) = \int_0^\infty e^{-ut}\check{w}_r(t). \tag{S70}$$

The bulk and boundary equations become,

$$\frac{1}{2}\left[\tilde{w}_{r+1}(u) + \tilde{w}_{r-1}(u)\right] - (1+u)\tilde{w}_r(u) = 0 \tag{S71}$$

$$\frac{1}{2}\tilde{w}_{2\nu}(u) - \left(\frac{1}{2}+u\right)\tilde{w}_\nu(s) + \nu\tilde{B}_\nu(u) = 0. \tag{S72}$$

The equation $\alpha^2 - 2(1+u)\alpha + 1 = 0$ has two solutions, but only one satisfies the condition $\alpha^r \underset{r\to\infty}{\to} 0$ imposed by Eq. (S68). The solution of Eq. (S71) is

$$\tilde{w}_r(u) = \gamma_\mu(u)\alpha^{|r|}, \tag{S73}$$

$$\alpha = 1 + u - \sqrt{(1+u)^2 - 1}, \tag{S74}$$

where μ is the sign of r. Injecting this expression into the boundary equation (S72), we obtain (recall that $\alpha^2 - 2(1+u)\alpha + 1 = 0$)

$$\gamma_\mu(u) = \frac{2\tilde{B}_\mu(u)}{(1+2u)\alpha - \alpha^2} = \frac{2\tilde{B}_\mu(u)}{1-\alpha} = \frac{2}{1-\alpha}\frac{(\partial_t\tilde{\psi})(u)}{e^{\mu\lambda}-1}. \tag{S75}$$

We finally use the velocity equation (S69) and obtain

$$(\partial_t \tilde{\psi})(u) = \frac{1}{2u}\left(e^{\lambda} + e^{-\lambda} - 2\right) - \frac{2\alpha}{1-\alpha}(\partial_t \tilde{\psi})(u), \tag{S76}$$

$$(\partial_t \tilde{\psi})(u) = \frac{1}{u}\frac{1-\alpha}{1+\alpha}\left[\cosh\lambda - 1\right] = \frac{1}{\sqrt{u(2+u)}}\left[\cosh\lambda - 1\right]. \tag{S77}$$

This expression can be inverted into

$$\partial_t \check{\psi}(t) = e^{-t} I_0(t)\left[\cosh\lambda - 1\right]. \tag{S78}$$

The large time limit is given by

$$\partial_t \check{\psi}(t) \underset{t\to\infty}{\sim} \frac{1}{\sqrt{2\pi t}}\left[\cosh\lambda - 1\right]. \tag{S79}$$

We also obtain the full solution for the generalized profiles $\tilde{w}_r$,

$$\tilde{w}_r(u) = \frac{1}{u}\frac{1}{1+\alpha}\left[1 - e^{-\mu\lambda}\right]\alpha^{|r|}. \tag{S80}$$

The small u behavior at constant $r\sqrt{u}$ gives the large time behavior at constant $r/\sqrt{t}$,

$$\tilde{w}_r(u) \underset{u\to 0}{\sim} \left[1 - e^{-\mu\lambda}\right]\frac{e^{-|r|\sqrt{2u}}}{2u} \tag{S81}$$

$$\check{w}_r(t) \underset{t\to\infty}{\sim} \frac{1}{2}\left[1 - e^{-\mu\lambda}\right]\operatorname{erfc}\left(\frac{|r|}{\sqrt{2t}}\right). \tag{S82}$$

III. GENERIC SINGLE-FILE SYSTEMS

A. Description of single-file systems in terms of two quantities

Two descriptions of single-file systems at large distance and large time have been put forward. They both involve two quantities.

The first description comes from fluctuating hydrodynamics [16]. The system considered is a lattice model. It is described at large distance and large time by a fluctuating density field $\rho(x,t)$ that is shown to obey the following equation,

$$\partial_t \rho(x,t) = \partial_x\left[D(\rho(x,t))\partial_x \rho(x,t) + \sqrt{\sigma(\rho(x,t))}\eta(x,t)\right]. \tag{S83}$$

The quantities $D(\rho)$ and $\sigma(\rho)$ were first defined from the microscopic details of a lattice gas [16]. It is nevertheless more intuitive to consider a system of size L between two reservoirs at densities ρ_a and ρ_b [2]. The number of particles transferred from left to right at time t is denoted Q_t and is shown to satisfy

$$\lim_{t\to\infty}\frac{\langle Q_t\rangle}{t} = \frac{D(\rho)}{L}(\rho_a - \rho_b) \quad \text{if } (\rho_a - \rho_b) \text{ is small,} \qquad \lim_{t\to\infty}\frac{\langle Q_t\rangle}{t} = \frac{\sigma(\rho)}{L} \quad \text{if } \rho_a = \rho_b = \rho. \tag{S84}$$

This can be used as a definition of $D(\rho)$ and $\sigma(\rho)$. Using macroscopic fluctuation theory (MFT), it has been shown [10] that the variance κ_2 of the displacement of a tagged particle in the system satisfies

$$\kappa_2 \underset{t\to\infty}{\sim} \frac{\sigma(\rho)}{\rho^2}\sqrt{\frac{t}{\pi D(\rho)}}. \tag{S85}$$

The second description has been developed by Kollmann [8]. The system consists of identical Brownian particles with pairwise interactions. Denoting the fluctuating density field $\rho(x,t)$, one defines the dynamical structure factor $S(q,t)$ as

$$S(q,t) = \frac{1}{N}\langle \delta\rho(q,t)\delta\rho(q,0)\rangle, \qquad \delta\rho(q,t) = \int dx\, e^{iqx}\left[\rho(x,t) - \bar{\rho}\right], \tag{S86}$$

where N is the number of particles and $\bar{\rho}$ the average density. The structure factor decays exponentially with time: $S(q,t) \sim S(q,0)e^{-D(q)t}$. The behavior of the system is shown to be dominated by the large wavelengths ($q \to 0$). The two important quantities (with their dependence on $\bar{\rho}$ written explicitly) are

$$D(\bar{\rho}) = \lim_{q\to 0} D(q), \qquad S(\bar{\rho}) = S(q=0, t=0). \tag{S87}$$

Kollmann shows that the mean square displacement of a tagged particle in the system satisfies

$$\kappa_2 \underset{t\to\infty}{\sim} \frac{2S(\rho)}{\rho}\sqrt{\frac{D(\rho)t}{\pi}}. \tag{S88}$$

Ref. [10] provides the link between the two approaches (Eq. (95)). $D(\rho)$ is the same quantity and $\sigma(\rho)$ and $S(\rho)$ are linked by $\sigma(\rho) = 2\rho D(\rho)S(\rho)$. Eqs. (S85) and (S88) are thus identical.

In the main text, we chose the description of Kollmann in terms of $D(\rho)$ and $S(\rho)$. We now list the values of these two quantities for the systems that we consider.

Model	$D(\rho)$	$S(\rho)$
Symmetric exclusion process [10]	D_0	$1-\rho$
Point-like hard core particles [10]	D_0	1
Pairwise interacting particles without hydrodynamic interactions [8, 14]	$\frac{D_0}{S(\rho)}$	$S(\rho)$
Hard rod gas [14]	$\frac{D_0}{(1-a\rho)^2}$	$(1-a\rho)^2$
Random average process [12]	$\frac{\mu_1}{2\rho^2}$	$\frac{\mu_2}{\mu_1-\mu_2}$

D_0 is the diffusion coefficient of an individual particle, a is the length of the hard rods, and μ_k are the moments of the probability law of the jumps in the RAP [12]. In the case of pairwise interacting particles, the structure factor $S(\rho)$ can either be determined directly from the positions, or indirectly from the pair correlations $g(r)$ via the compressibility relation [4],

$$S(\rho) = \lim_{q\to 0}\frac{1}{N}\left\langle \sum_{i,j} e^{iq(X_i - X_j)}\right\rangle = 1 + \int_{-\infty}^{\infty} dr\,[g(r)-1]\,. \tag{S89}$$

B. Extension of our approach

In light of the description in terms of the two quantities $D(\rho)$ and $S(\rho)$, we extend Eqs. (S20)-(S23) to generic single-file systems.

$$D(\rho)\Phi_1''(v) + v\Phi_1'(v) = 0, \tag{S90}$$

$$D(\rho)\Phi_1'(0^\pm) + \frac{1}{2}\rho\tilde{\kappa}_2 = 0, \tag{S91}$$

$$\Phi_1(0^+) - \Phi_1(0^-) = S(\rho), \tag{S92}$$

$$\Phi_1(v) \xrightarrow[v\pm\infty]{} 0, \tag{S93}$$

with ρ the average density of the system. We recall that for the SEP, we had $D(\rho) = 1/2$ and $S(\rho) = 1-\rho$.

The solution is readily obtained:

$$\Phi_1(v \gtrless 0) = \pm\frac{S(\rho)}{2}\,\mathrm{erfc}\left(\frac{|v|}{\sqrt{2D(\rho)}}\right), \tag{S94}$$

$$\tilde{\kappa}_2 = \frac{S(\rho)}{\rho}\sqrt{\frac{2D(\rho)}{\pi}}. \tag{S95}$$

We stress that this solution is exact, as confirmed by the alternative derivation provided in Section III C.

If we call $\eta(x,t)$ the density field at x at time t and X_t the position of the tracer at time t, this means

$$\langle \eta(X_t+x,t)X_t\rangle \underset{t\to\infty}{\sim} \mathrm{sign}(x)\frac{S(\rho)}{2}\,\mathrm{erfc}\left(\frac{|x|}{\sqrt{4D(\rho)t}}\right) \tag{S96}$$

$$\left\langle X_t^2\right\rangle \underset{t\to\infty}{\sim} \frac{S(\rho)}{\rho}\sqrt{\frac{4D(\rho)t}{\pi}}. \tag{S97}$$

The result for the variance is the one given in Refs [8, 10].

C. MFT

In the formalism of Macroscopic Fluctuation Theory (MFT), the main object is the density $\rho(x,\tau)$ which is the continuous equivalent of the occupation $\eta_i(t)$ at time $t=\tau T$, $\tau\in[0,1]$ with $x=i/\sqrt{T}$. The probability to start from a density ρ_0 at $t=0$ and end up with a density $\rho(x,1)$ at $t=T$ is given by [3]:

$$\mathbb{P}(\rho_0(x)\longrightarrow\rho(x,1)) = \int \mathcal{D}[\rho(x,\tau)]\mathcal{D}[H(x,\tau)]\,\mathrm{e}^{-\sqrt{T}\,S[\rho,H]}\,, \tag{S98}$$

where the action S reads

$$S[\rho,H] = \int \mathrm{d}x\int_0^1 \mathrm{d}\tau\left(H\partial_\tau\rho+\frac{1}{2}\partial_x\rho\partial_x H-\frac{\rho(1-\rho)}{2}(\partial_x H)^2\right)\,. \tag{S99}$$

The distribution of the initial condition ρ_0 takes the form

$$\mathbb{P}[\rho_0]\simeq \mathrm{e}^{-\sqrt{T}\,F[\rho_0]}\,, \tag{S100}$$

where

$$F[\rho(x,0)] = \int \mathrm{d}x\int_\rho^{\rho(x,0)}\mathrm{d}z\,\frac{\rho(x,0)-z}{z(1-z)}\,. \tag{S101}$$

The cumulant generating function for the position of the tracer can be written as [11]

$$\left\langle \mathrm{e}^{\lambda X_T}\right\rangle \simeq \int \mathcal{D}\rho_0\int \mathcal{D}[\rho(x,\tau)]\mathcal{D}[H(x,\tau)]\,\mathrm{e}^{-\sqrt{T}\,(S[\rho,H]+F[\rho_0]-\lambda Y[\rho])}\,, \tag{S102}$$

where $Y[\rho]=X_T/\sqrt{T}$ is the position of the tracer. It is deduced from $\rho(x,\tau)$ from the conservation of the number of particles to the right of the tracer:

$$\int_0^{Y[\rho]}\rho(x,1)\mathrm{d}x = \int_0^\infty\left(\rho(x,1)-\rho(x,0)\right)\mathrm{d}x\,. \tag{S103}$$

For large T, the integral in (S102) is dominated by the minimum of $S+F-\lambda Y$, taken as a function of (ρ,H). We denote this minimum (q,p). These functions satisfy the equations [11]

$$\partial_\tau q = \partial_x[D(q)\partial_x q]-\partial_x[\sigma(q)\partial_x p]\,, \tag{S104}$$

$$\partial_\tau p = -D(q)\partial_x^2 p-\frac{1}{2}\sigma'(q)(\partial_x p)^2\,, \tag{S105}$$

with the terminal condition for p

$$p(x,\tau=1) = B\Theta(x-Y)\,,\quad B=\frac{\lambda}{q(Y,1)}\,, \tag{S106}$$

and the initial condition for q, expressed in terms of $p(x,0)$:

$$p(x,0) = B\Theta(x)+\int_\rho^{q(x,0)}\mathrm{d}r\,\frac{2D(r)}{\sigma(r)}\,. \tag{S107}$$

This approach has been used to compute the first four cumulants of the position of the tracer [11].

We can make a connection between this approach and the generalized profiles, since the latter can be expressed as

$$w_r(\lambda,T) = \frac{\left\langle \eta_{X_T+r}(T) \mathrm{e}^{\lambda X_T} \right\rangle}{\left\langle \mathrm{e}^{\lambda X_T} \right\rangle} \simeq \frac{\displaystyle\int \mathcal{D}\rho_0 \int \mathcal{D}[\rho(x,\tau)]\mathcal{D}[H(x,\tau)]\, \rho(r/\sqrt{T}+Y[\rho],1)\, \mathrm{e}^{-\sqrt{T}\,(S[\rho,H]+F[\rho_0]-\lambda Y_T[\rho])}}{\displaystyle\int \mathcal{D}\rho_0 \int \mathcal{D}[\rho(x,\tau)]\mathcal{D}[H(x,\tau)]\, \mathrm{e}^{-\sqrt{T}\,(S[\rho,H]+F[\rho_0]-\lambda Y_T[\rho])}} \,. \tag{S108}$$

The two integrals can be evaluated via a saddle point method. The saddle point is the same for the numerator and the denominator and is given by (q,p) solution of (S104,S105). Therefore, for large T,

$$w_r(\lambda,T) \simeq q\left(\frac{r}{\sqrt{T}} + Y[q], \tau=1\right) . \tag{S109}$$

In our formalism we have $v = r/\sqrt{2T}$, thus,

$$\Phi(v) = q(v\sqrt{2} + Y[q], \tau=1) - \rho \,, \tag{S110}$$

which relates our generalized profiles to the MFT solution.

The MFT equations (S104,S105) can be solved perturbatively at first order in λ. Let us denote

$$q(x,\tau) = \rho + \lambda\, q_1(x,\tau) + \cdots \,, \tag{S111}$$
$$p(x,\tau) = \lambda\, p_1(x,\tau) + \cdots \,. \tag{S112}$$

We also write the expansion of $Y[q]$:

$$Y = Y_0 + \lambda\, Y_1 + \cdots \,. \tag{S113}$$

The coefficients can be determined via the condition (S103) which yields

$$\rho Y_0 = 0 \,, \tag{S114}$$
$$\rho Y_1 = \int_0^\infty (q_1(x,1) - q_1(x,0))\, \mathrm{d}x \,. \tag{S115}$$

The boundary conditions (S106,S107) give a series of conditions for the p_i's and q_i's. At first order, we get

$$p_1(x,1) = \frac{1}{\rho}\Theta(x) \,, \tag{S116}$$
$$q_1(x,0) = \frac{\sigma(\rho)}{2D(\rho)}(p_1(x,0) - \rho^{-1}\Theta(x)) \,, \tag{S117}$$

and the MFT equations (S104,S105) become

$$\partial_\tau q_1 = D(\rho)\partial_x^2 q_1 - \sigma(\rho)\partial_x^2 p_1 \,. \tag{S118}$$
$$\partial_\tau p_1 = -D(\rho)\partial_x^2 p_1 \,, \tag{S119}$$

We first solve the equation for p_1 and then use the result to solve the equation for q_1. This gives, at $\tau = 1$:

$$q_1(x,\tau=1) = \frac{\sigma(\rho)}{4\rho D(\rho)} \operatorname{sign}(x) \operatorname{erfc}\left(\frac{|x|}{\sqrt{4D(\rho)}}\right) . \tag{S120}$$

From (S110), we deduce

$$\Phi_1(v) = \frac{\sigma(\rho)}{4\rho D(\rho)} \operatorname{sign}(v) \operatorname{erfc}\left(\frac{|v|}{\sqrt{2D(\rho)}}\right) , \tag{S121}$$

which is exactly (S94).

IV. NUMERICAL SIMULATIONS

A. Symmetric exclusion principle

Simulations of the SEP are performed on a periodic ring of size $N = 1000$. The average density is set to ρ and $M = \rho N$ particles are initially placed uniformly at random on the ring. The successive jumps of the particles are implemented as follow: one chooses a particle uniformly at random and one of the two possible directions (left and right) with equal probabilities. If the chosen particle has no neighbor in the chosen direction, the jump is performed, else it is rejected. In both cases, the time of the simulation is incremented by a random number drawn according to an exponential distribution of rate N.

We keep track of one particle (the tracer) and compute its moments and the generalized profiles at the times that we want. The average is taken over 10^8 repetitions of the simulation.

B. Point-like hard-core diffusive particles

We consider particle that diffuse on a line, with hard-core exclusions. One notes that the dependence in the density is trivial since at density ρ the space x and the time τ can be rescaled as $x \leftarrow \rho x$ and $\tau \leftarrow \rho^2 \tau$. We thus consider only $\rho = 1$. Initially ($\tau = 0$), $M = 20001$ particles are placed uniformly at random on the interval $[0, M]$. The tracer is particle number $(M + 1)/2$. We consider that the particles diffuse independently of one another, then we implement the hard core interactions by restoring the order. Practically, between time 0 and τ, particle k moves by Δx_i drawn according to the Gaussian probability law

$$P(\Delta x_k, \tau) = \frac{1}{\sqrt{2\pi\tau}} e^{-\frac{(\Delta x_k)^2}{2\tau}}. \tag{S122}$$

The tracer is still particle number $(M + 1)/2$ from the left. Its displacement and the density field in its reference frame are easily computed. To compute the observables, the average is performed over $4 \cdot 10^8$ repetitions.

C. Hard-rod gas

We consider a gas of diffusive hard rods of size $a < 1$ at density $\rho = 1$. The position of rod k at time t is denoted $y_k(t)$. We may substract the rod sizes from the positions and define $x_k(t) = y_k(t) - ka$. One realizes that the set $\{x_k(t)\}$ correspond to point-like hard-core diffusive particles. Using the mapping $y_k(t) = x_k(t) + ka$ at both the initial and final times, one can compute the observables of the hard-rod gas from simulations of the point-like particles described above.

The low-density limit of the model correspond exactly to the point-like hard-core diffusive particles. In this case, the profiles at order 2 and 3 are given in Fig. 3 of the article.

D. Random-average process

We consider the random-average process (RAP) defined in particular in Ref. [12]. Particles are placed on the infinite one-dimensional line. They are all embedded with exponential clocks of characteristic time 1. When its clock ticks a particle jumps choose a direction, left or right, with equal probability. It then jumps in this direction at a distance which corresponds to a fraction η of the distance to its nearest neighbor. η is a random variable following a probability law on $[0, 1]$. In our simulations, we choose the uniform probability law.

By construction of the RAP, if the density of the particles is denoted ρ and if x and t are respectively the spatial and temporal coordinates, the observables depend only on the two rescaled coordinates $z = \rho x$ and $\tau = \rho t$. For this reason, we only consider the RAP at density $\rho = 1$.

In our simulations, we consider $N = 500$ particles on a periodic line (of length $L = 500$). The steady state of the RAP is non-trivial [12] and can hardly be implemented as an initial condition. We thus first let the system evolve for a time $t_{\text{ini}} = 2 \cdot 10^4$ before starting to record the observables. These observables are then averaged over $2 \cdot 10^6$ simulations.

Note that the low-density limit of the RAP is peculiar since $S(\rho) \sim \rho^{-1}$. It does not correspond to the ideal gas ($S(\rho) = 1$). Therefore, the profiles at order 2 cannot be checked against our low-density prediction.

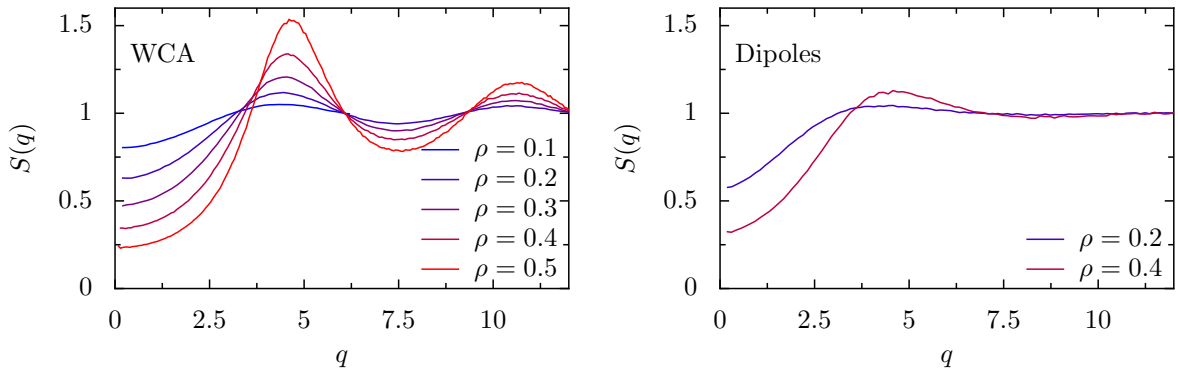

ρ	0.1	0.2	0.3	0.4	0.5
$S(\rho) = S(q=0)$	0.82	0.63	0.48	0.35	0.23

ρ	0.2	0.4
$S(\rho) = S(q=0)$	0.58	0.32

FIG. S1. Structure factor $S(q)$ and measured value of $S(\rho) = S(q = 0)$. Left: WCA potential. Right: dipole-dipole potential.

E. Point-like particles interacting by a pairwise potential

We consider N particles ($N = 500$ for WCA potential, $N = 200$ for dipole-dipole potential) on a ring of length $L = N/\rho$ where ρ is the density. The particles diffuse with a diffusion coefficient $D_0 = 1$. In addition, they interact by a pair potential $V(r)$. Two kinds of interactions are considered: a short-range WCA potential $V_{\mathrm{WCA}}(r)$ and a long-range dipole-dipole potential $V_{\mathrm{dip}}(r)$,

$$V_{\mathrm{WCA}}(r) = \begin{cases} 4A_{\mathrm{WCA}}\left(\frac{1}{r^{12}} - \frac{1}{r^6}\right) & r < 2^{1/6} \\ 0 & r > 2^{1/6} \end{cases}, \qquad V_{\mathrm{dip}}(r) = \frac{A_{\mathrm{dip}}}{r^3}, \tag{S123}$$

with $A_{\mathrm{WCA}} = A_{\mathrm{dip}} = 1$. In the case of the dipole-dipole interaction, we consider that the ring is a circle of radius $L/(2\pi)$ embedded in 2d space: the distance r between two particle is the distance between the points of the circles so that the 1d force is the tangential component of the 2d force.

The time-step for the Brownian dynamics is set to $\Delta t = 2 \cdot 10^{-4}$. Starting from random initial positions, we let the system equilibrate during a time $t_0 = 10^4$ before recording the observables. At each iteration, we check that the particles are ordered and if they are not, we restart the simulation ($< 1\%$ of simulations in the worst case). To regularize the diverging potentials at small distance, we ensure a maximum displacement of a particle during a time iteration (0.1 units ; only a frequency $\sim 10^{-7}$ of the moves need this regularization). We average the results over 50000 simulations (WCA potential) or 2500 simulations (dipole-dipole potential).

The structure factor $S(q)$ used in Fig. 4 of the article is computed by the two methods of Eq. (S89) (we check that they are consistent). The graphics and the table of values are given in Fig. S1.

[1] Richard Arratia. The motion of a tagged particle in the simple symmetric exclusion system on z. *The Annals of Probability*, 11(2):362–373, 05 1983.

[2] Bernard Derrida. Non-equilibrium steady states: fluctuations and large deviations of the density and of the current. *Journal of Statistical Mechanics: Theory and Experiment*, 2007(07):P07023, 2007.

[3] Bernard Derrida and Antoine Gerschenfeld. Current fluctuations in one dimensional diffusive systems with a step initial density profile. *Journal of Statistical Physics*, 137(5-6):978–1000, 2009.

[4] Jean-Pierre Hansen and Ian Ranald McDonald. *Theory of simple liquids: with applications to soft matter*. Academic Press, 2013.

[5] Chaitra Hegde, Sanjib Sabhapandit, and Abhishek Dhar. Universal large deviations for the tagged particle in single-file motion. *Physical Review Letters*, 113(12), sep 2014.

[6] P. Illien, O. Bénichou, C. Mejía-Monasterio, G. Oshanin, and R. Voituriez. Active transport in dense diffusive single-file systems. *Phys. Rev. Lett.*, 111:038102, Jul 2013.

[7] Takashi Imamura, Kirone Mallick, and Tomohiro Sasamoto. Large deviations of a tracer in the symmetric exclusion process. *Physical Review Letters*, 118(16):160601–, 04 2017.

[8] Markus Kollmann. Single-file diffusion of atomic and colloidal systems: Asymptotic laws. *Phys. Rev. Lett.*, 90(18):180602, May 2003.

[9] P. L. Krapivsky, Kirone Mallick, and Tridib Sadhu. Large deviations in single-file diffusion. *Phys. Rev. Lett.*, 113(7):078101, Aug 2014.

[10] P L Krapivsky, Kirone Mallick, and Tridib Sadhu. Dynamical properties of single-file diffusion. *Journal of Statistical Mechanics: Theory and Experiment*, 2015(9):09007, sep 2015.

[11] Paul L Krapivsky, Kirone Mallick, and Tridib Sadhu. Tagged particle in single-file diffusion. *Journal of Statistical Physics*, 160(4):885–925, 2015.

[12] A. Kundu and J. Cividini. Exact correlations in a single-file system with a driven tracer. *EPL (Europhysics Letters)*, 115(5):54003, sep 2016.

[13] C. Landim, S. Olla, and S. B. Volchan. Driven tracer particle in one dimensional symmetric simple exclusion. *Communications in Mathematical Physics*, 192(2):287–307, 03 1998.

[14] Binhua Lin, Mati Meron, Bianxiao Cui, Stuart A. Rice, and Haim Diamant. From random walk to single-file diffusion. *Phys. Rev. Lett.*, 94(21):216001, jun 2005.

[15] Tridib Sadhu and Bernard Derrida. Large deviation function of a tracer position in single file diffusion. *Journal of Statistical Mechanics: Theory and Experiment*, 2015(9):P09008, sep 2015.

[16] H Spohn. Long range correlations for stochastic lattice gases in a non-equilibrium steady state. *Journal of Physics A: Mathematical and General*, 16(18):4275–4291, dec 1983.